International Journal of Mechanical Engineering and Applications
2021; 9(6): 98-112
http://www.sciencepublishinggroup.com/j/ijmea
doi: 10.11648/j.ijmea.20210906.13
ISSN: 2330-023X (Print); ISSN: 2330-0248 (Online)

Effective Folding Line Processing with a Press Method in Origami Forming Using a Low-cost and Simple V-shaped Punch Tool System

Kosuke Terada[1, *], Ichiro Hagiwara[2]

[1]Department of Mechanical Engineering, School of Science and Engineering, Meisei University, Hino-city Tokyo, Japan

[2]Meiji Institute for Advanced Study of Mathematical Sciences, Meiji University, Tokyo, Japan

Email address:

kosuke.terada@meisei-u.ac.jp (K. Terada), ihagi@meiji.ac.jp (I. Hagiwara)

[*]Corresponding author

To cite this article:

Kosuke Terada, Ichiro Hagiwara. Effective Folding Line Processing with a Press Method in Origami Forming Using a Low-cost and Simple V-shaped Punch Tool System. *International Journal of Mechanical Engineering and Applications*. Vol. 9, No. 6, 2021, pp. 98-112.
doi: 10.11648/j.ijmea.20210906.13

Received: November 25, 2021; **Accepted**: December 10, 2021; **Published**: December 24, 2021

Abstract: Bent products have recently been applied widely in various structures. The method of sharp bending has the advantage of producing bent products with a fine appearance. Meanwhile, it has been recently shown that origami forming can be applied as a free manufacturing method that creates a fine appearance using complex folding lines. Sharp bending and origami forming both require folding lines. Folding lines are produced to make a V-groove before bending. Cutting V-grooves for folding lines requires machining center plants and long working times, which are not suitable for mass production. This paper presents newly developed and convenient V-shaped punch tools for folding line processing in sharp bending and origami forming. As a result, origami forming is expected to be adopted as a press method using V-shaped punch tools. Additionally, this paper reports on the findings of deformation behavior and mechanism obtained in experiments on folding line processing. The investigation for three-dimensional plate deformation around the V-shaped punch terminal shows extended folding line by terminal effect. Phenomena and the required load of V-shape punch indentation are considered in determining the mechanism of V-shape punch indentation from the results of finite element analyses and experiments on groove formation using V-shaped punch tool system.

Keywords: Sharp Bending, V-shaped Punch, Press, Mechanism, FEM, Origami Forming

1. Introduction

There are many bent products, such as those used in construction, automobiles, and home appliances. From the point of view of aesthetics, products with sharp bending angles are appealing. Cutting a V-groove along the inside of a bend in advance and sharply bending the flat material along this groove is one method for creating bent products. However, equipment such as a computer numerically controlled (CNC) router or machining center is required for cutting and such equipment is not suitable for mass production owing to the long cutting time. To solve this problem, Ogawa and Makinouchi [1] proposed a method whereby a V-shaped punch is first pushed by a press as a forging method and bending is then performed after V-groove processing on the folding lines. They reported that bending is easier when using their proposed method than when using the cutting method and the manufacturing process is greatly streamlined. Moreover, they reported that benefits such as improved product strength can be achieved through strain hardening by the pressing action in forging. Meanwhile, in recent years, we have advocated a method called origami forming whereby products of various shape can be manufactured with a short delivery time [2–6]. The bent product obtained using this method is similar to that obtained in sharp bending. Origami forming products have many folding lines, a number of which intersect as shown in Figure 1 [3]. However, tools used in V-grooving (hereinafter referred to as folding line processing) to form the folding lines required in origami forming with the punch shape used by Ogawa and Makinouchi are not readily available. Despite the pioneering reports of the benefits of easy sharp bending after grooving, the mechanism of plate deformation has not been discussed.

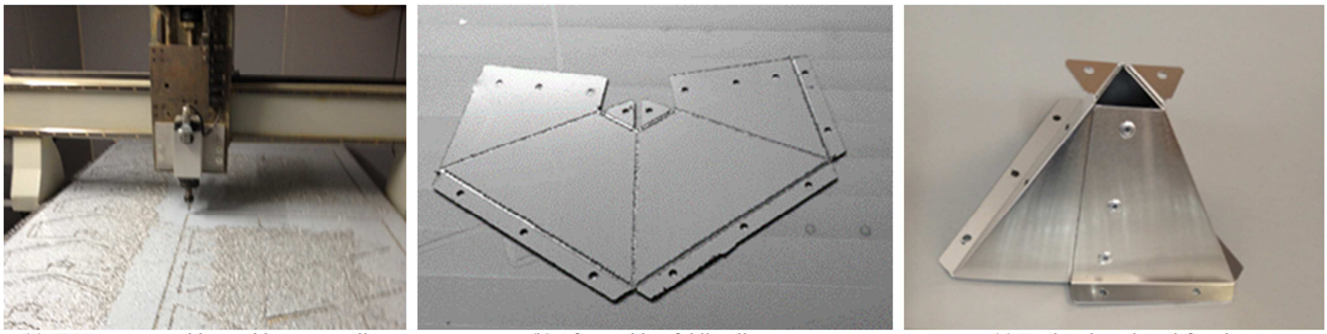

(a) CNC router machine making groove lines (b) After making folding lines (c) Product by origami forming

Figure 1. *Origami forming based on folding lines by CNC router machine for making groove lines.*

The practical use of folding line processing by pressing with a V-shaped punch requires the establishment of not only the forming conditions for folding line processing targeting many materials and processed product shapes but also the design technology for jig tool system. It is also important to examine the mechanism and to clarify the technical issues to be tackled. This paper proposes folding line processing using a low-cost and simple V-shaped punch tool system with a press method that can be used in sharp bending and origami forming. The paper also discusses the mechanisms of changes in plate material and plate thickness in folding line processing based on findings obtained by experiments and FEM results.

2. Types and Importance of Folding Line Processing Methods

As described in previous papers [3-6], sharp bending is facilitated by performing folding line processing in advance with grooves having a width of approximately the plate thickness and a depth of approximately half the plate thickness. Although it is a feature of origami forming, it cannot be sharply bent without folding line processing. If the cutting method is used for folding line processing, equipment such as a CNC router or machining center is required and such equipment is not suitable for mass production because of the long cutting time. Here, mass production refers to a monthly production level of 10,000 pieces. This means that folding line processing for one piece must be finished within 1 minute assuming that the monthly operating hours are 9600 minutes ((20 days × 8 hours per day) × (60 minutes per hour) = 9600 minutes and 10,000 pieces per 9600 minutes ≅ 1 minute per 1 piece). Considering the cutting time required for the drill bit to move along the folding line, it is difficult to cut one piece within 1 minute if that piece has a folding line length of several hundred millimeters or more. Although there is also a method of grooving for folding lines using laser irradiation, this method faces the same problem as the cutting method considering the time for the laser beam to move along a folding line. Meanwhile, grooving by forging with a press to reduce the thickness of the folding lines involves one movement upward and downward of the die even for large products with very long folding lines and, as a result, the press working time is within 1 minute and is suitable for mass production.

Next, the jig tool system design is an issue for folding line processing. The dimensions of a V-shaped punch with a rounded tip that Ogawa et al. used for push-in groove processing using a CNC turret punch press were 5 mm (thickness) × 30 mm (height). It is difficult to use such a tool shape for products having multiple folding lines that intersect. In Figure 2, three folding lines intersect at an angle of 60° with a gap at the intersection, and processing such that the three folding lines are continuous using the punch with the above dimensions increases the cost.

Moreover, using this punch, the block material is processed for each folding line such that the production cost increases when there are many fold lines. The technology may be profitable even though the design and production costs are high if the production tooling and press die are for an ordered product. However, it is necessary to devise design specifications of a V-shaped punch that can be used inexpensively for experiments/prototypes with many folding lines, a number of which intersect. Against the above background, this paper proposes design specifications of a V-shaped punch for pressing (forging) as shown in Figures 3–5.

First, V-shaped groove cutting is performed on the block material. Next, a V-shaped punch with a square cross section is set in the groove. A smaller square cross-section results in a smaller folding line pitch. However, the punch will break during producing V-shaped punches if the square cross-section is too small. A V-shaped punch with this feature is manufactured without heat treatment by cutting out a rod shape (2 mm × 2 mm × 65 mm) from commercial high-speed steel material (SK5; 2 mm × 5 mm × 65 mm) in a milling process as shown in Figure 3(a). The dimensions of the square cross-section of rod are the minimum processing size, with one or two pieces cracking if 20 pieces are manufactured. After making this V-shaped punch and confirming the function of the groove, the corner R of the square cross-section is measured with a microscope and finished to R = 0.2 mm in Figure 5. Microscopic measurements made after the folding line processing experiment indicate that the shape is retained. Figures 3 and 4 show a groove with dimensions of 150 mm

(length) × 2.8 mm (width) × 1.4 mm (depth) machined in the center of a high-speed steel (SKD11) block with dimensions of 50 mm × 50 mm × 150 mm by a V-shaped cutter (FX-MG-VCM90°) and V-shaped punch with dimensions of 65 mm (length) × 2 mm × 2 mm (cross section) is set in this center groove. The block size was set for ease of experimentation. The V-shaped punch has a width δ of 2.8 mm and tip height of approximately 1.4 mm, which was set after grooving the block material for the bed. The proposed method can be applied even for pieces with many fold lines and intersections of the fold lines at low cost as follows.

Figure 6 shows a processed product having an octahedron half core shape and an aluminum thickness of 1.0 mm as a prototype example. It has been reported [7-9] that it is difficult theoretically to make a core of steel with an aspect ratio of 0.28 or more through press forming, where the aspect ratio is defined as the ratio $f = h/c$ of the height h to the top of the tip of the triangular or quadrangular pyramid to the length c of one side of the bottom surface. The aspect ratio of the processed product shape in Figure 6 is $f = 0.71$ by the above definition, and the shape is thus difficult to form through press forming. However, the shape is easily formed through the proposed origami forming. But even the very high aspect core is easily formed by this proposing origami forming which is expected to be used as a sound insulation core, because a core with high aspect ratio is effective as a sound insulation structure with the sound absorbing material set on the top surface side [10, 11].

In a previous paper [4], sound insulation parts were formed through origami forming by fold line processing using a machining center. Here, however, fold lines are processed using a press. In the bottom flange of this part, three punch-width lines (WL-1, 2, 3) cross (○ symbol in Figure 6 (c)). The case the proposed V-shaped punch is applied in this folding line processing is explained as follows.

HJ represents the punch terminal line set along WL-1, CE as the punch terminal line set along WL-2, JL as the punch terminal line set along WL-3, δ as the punch width, and O as the intersection of the three center lines of the punch-width lines. The distance that the V-shaped punch cannot reach owing to the interference of the WL-1 and WL-2 tools is DJ = 0.289δ. Punch terminal lines are the cutting lines for the left and right flanges. In the case of the proposed tool, the punch width is δ = 2.8 mm and DJ ≅ 0.8 mm. If the total length is several tens of millimeters, as described below, three folding lines (FL-1, 2, 3) approach the intersection after folding line processing and, as a result, sharp bending is possible via the effect of the three-dimensional deformation behavior of the plate material around the V-shaped punch terminal (hereinafter called the terminal effect). The enlarged photograph in Figure 6(f) shows that the terminal position of folding line FL-2 generated by folding line processing is near folding lines FL-1 and FL-3. In the case of thickness of 1 mm, such that the groove width is 1 mm for FL-1, 2, and 3, three folding lines approach the intersection, and there is no 0.8 mm gap shown in the photograph. This processing procedure is described as follows.

1) Perform V-shaped groove processing for eight lines as setting V-shaped punches along using a V-shaped cutter on a high-speed steel (SKD11) block material having dimensions of 200 mm × 200 mm × 20 mm in Figure 6(c).
2) Set eight high-speed-steel rod-shaped V-shaped punches with cross-sectional dimensions of 2 mm × 2 mm on the folding lines in Figure 6(d).
3) Insert the plate material on the set V-shaped punches (Figure 6(e)) and perform folding line processing by applying a predetermined load with a press machine. The predetermined load required for the folding lines of various products should be calculated such that the indentation load required per unit length of the folding line is suitable for various materials/plate thicknesses. Results of the analysis of the indentation load setting method and plate deformation mechanism from experiments and finite element method (FEM) analysis are presented from section 3.
4) Bend the plate along the folding lines after folding line processing (Figure 6(f)). Even at the intersection of three folding lines, the flange surface can be sharply bent as shown in the photograph (Figure 6(f)). This paper proposes a principle-based method of folding line processing using a press. In the post process, manual bending is performed using a gripper. Actual mass production requires durable jigs and tools and an automatic bending method having a mechanism and machining conditions that meet the target dimensional accuracy range. These developments are left as future tasks.

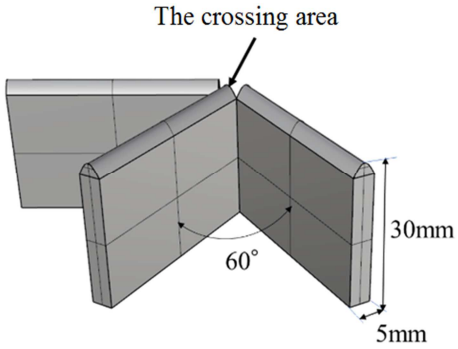

Figure 2. *Crossing three V-shaped punches (depth 5 mm×height 30 mm).*

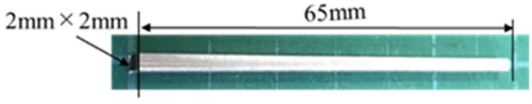

(a) V-shaped punch (2mm×2mm×65mm)

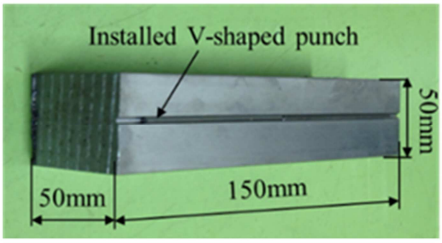

(b) Installed punch in bed (50mm×50mm×150mm)

Figure 3. *V-shaped punch tool design style.*

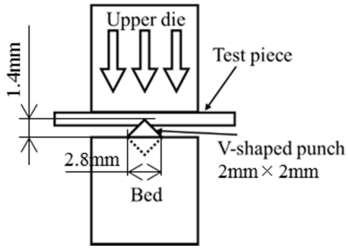

Figure 4. *V-shaped punch in bed and pressed test piece by hydraulic system universal testing machine.*

Meanwhile, in the tool specifications shown in Figure 2, owing to the punch width δ = 5 mm, the folding line length that has not formed is about 1.5 mm according to the relational expression obtained in Figure 6(b); this length is about twice that of the proposed punch. There are thus restrictions concerning the shapes and dimensions in the punch specifications in Figure 2. Although the proposed forming method has almost no design cost and the production cost is tens of thousands of yen, in the case of the punch specifications in Figure 2, it is estimated that the production cost including the part/die structural design cost, process design cost, part/material costs, and machining cost is about 10 times higher because punches are machined for each folding line and an attachment is required to assemble and integrate all tools. The above design specifications of the V-shaped punch of the proposed technology can be applied to cores having a high aspect ratio that cannot be formed using press methods and can also be applied to cores having many folding lines and the intersection of multiple folding lines in Figure 6. Moreover, the proposed technology has important advantages, such as good working efficiency and low costs.

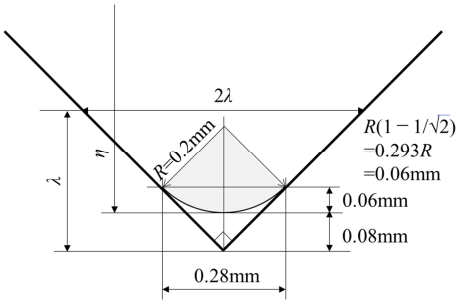

Figure 5. *V-shaped punch tip and definition of λ and η.*

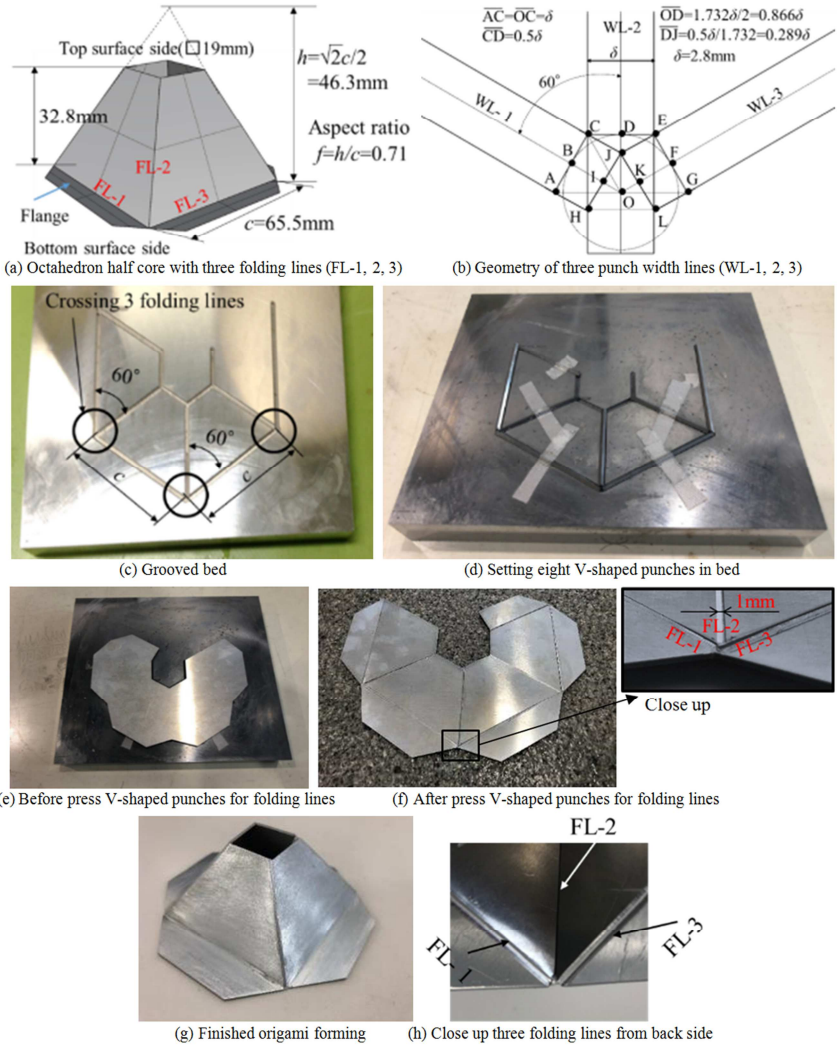

(a) Octahedron half core with three folding lines (FL-1, 2, 3)

(b) Geometry of three punch width lines (WL-1, 2, 3)

(c) Grooved bed

(d) Setting eight V-shaped punches in bed

(e) Before press V-shaped punches for folding lines

(f) After press V-shaped punches for folding lines

(g) Finished origami forming

(h) Close up three folding lines from back side

Figure 6. *Origami forming trial product (Aluminum t=1.0mm) success by using V-shaped punch tool system. Three ○ show crossing three folding lines. Good origami forming could be done even at ○ locations.*

3. Experiment Method • Results

3.1. Test Pieces and Folding Line Processing Experiments

Test pieces used in the experiments were cold-rolled mild-steel sheets with thickness t = 0.4, 0.6, and 0.8 mm and aluminum plates (A1050P) with thickness t = 0.4, 0.6, 0.8, and 1.0 mm. A manufacturing test piece was finished through deburring and polishing after being cut to a size of 50 mm × 150 mm using a shearing machine. Table 1 gives the standard material constants of the test pieces, namely the Young modulus E, plasticity coefficient F, strain hardening index n, Poisson ratio v, and yield stress σ_y [15].

As shown in Figure 4, an indentation load P was loaded to the test piece by a universal testing machine (SHIMAZDU, UH-F500kNI) after the test piece was inserted between the V-shaped punch and upper die. P is the indentation load required for the V-shaped punch to make an indentation of 1 mm into the test piece per unit folding line length of 1 mm. The descent speed of the upper die was set at 0.6 mm/min to prevent any disturbance. However, it is difficult to adjust P by directly measuring the groove depth in setting P required for an indentation of 1 mm per unit folding line length of 1 mm. Therefore, assuming that the groove depth equals the size of the V-shaped punch indentation, the indentation made by the V-shaped punch λ was calculated approximately as $\lambda = 0.5\lambda_s$ (where λ_s denotes the measurement of the surface imprint length) at the working site of the laboratory. This calculation is based on the geometric relationship shown in Figure 5; i.e., the surface imprint length of the test piece is twice λ because of the cross-sectional shape of the V-shaped punch being square as shown in Figure 3. However, there are errors in this calculation method for the following reasons. The real tip of the V-shaped punch has a radius of 0.2 mm and is not a square shape. Therefore, the real tip is 0.08 mm smaller than the square shape. Only the tip arc enters the plate before the V-shaped punch indents to a depth of 0.06 mm, finally the geometric relationship of the square shape appears after the V-shaped punch indents to a depth of more 0.06 mm.

As shown in Figure 7, measurements based on micrographs of the formed test piece provide not only λ_s but also λ_b in the folding line processing experiments using mild steel and aluminum test pieces because when the surface imprint length λ_s of the concave part on the surface side of the test piece is measured, the surface imprint length λ_b of the convex part is clearly confirmed on the plate back surface also. Table 2 gives measurements made three times for the micrographs under each condition, as for surface imprint length measurements.

Experimental data are obtained to judge whether the V-shaped punch has indented to approximately half the plate thickness when λ_s almost reaches the plate thickness. The folding line processing experiments using mild steel and aluminum test pieces are performed at various P. All measurements are presented in Table 2 and Figure 8. The measurements in Figure 8 show that both λ_b and λ_s are largely proportional to P for both mild steel and aluminum test pieces.

Table 1. *Material constants of Mild steel (SPCC) and Aluminum (A1050P).*

Symbol	Mild steel	Aluminum
E(GPa)	206	70
F(MPa)	627	153
n(-)	0.25	0.25
v(-)	0.30	0.30
σ y (MPa)	200	70

Table 2. *Measured data of λ_s and λ_b.*

(a) Mild steel (SPCC)

t(mm)	P(N/mm)	λs (μ mm)	λb (μ mm)
0.4	150	168	720
		164	700
		164	720
	300	419	869
		419	839
		419	854
0.6	450	639	1224
		641	1195
		642	1230
0.8	600	900	1758
		902	1758
		900	1709

(b) Aluminum (A1050P)

t(mm)	P(N/mm)	λs (μ mm)	λb (μ mm)
0.4	80	398	808
		400	786
		397	801
	100	503	885
		500	869
		498	877
0.6	160	700	1712
		696	1705
		692	1678
0.8	160	700	1641
		692	1660
		687	1644
1.0	200	894	2067
		888	2112
		885	2105
	240	1213	2501
		1214	2539
		1222	2486

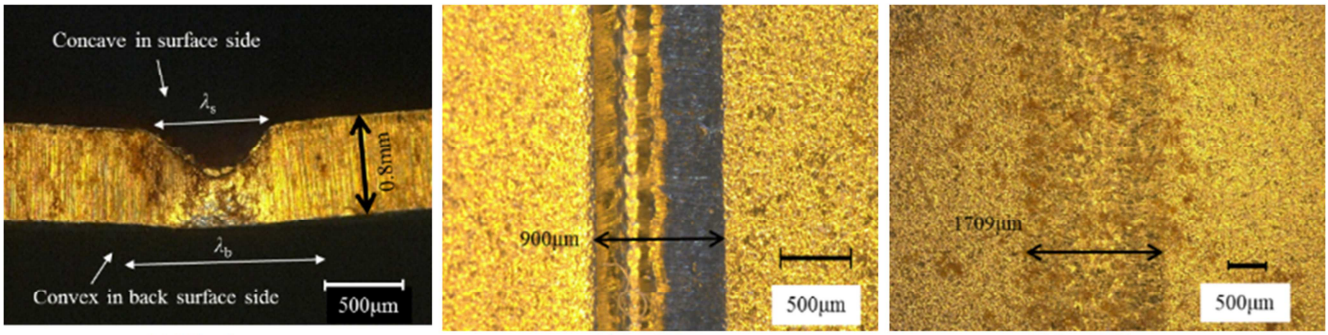

(a) Side view (b) λ_s = 900 μm (c) λ_b =1709 μm

Figure 7. *Surface imprint length λ_s and λ_b in grooved mild steel piece t=0.8 mm, P=600 N/mm.*

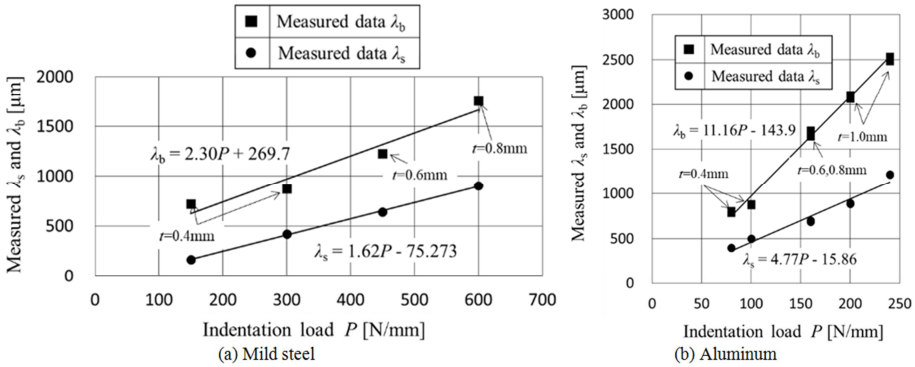

Figure 8. *Relationship between measured data λ_b, λ_s and indentation load P.*

3.2. Evaluation of Sharp Bending Formability and Shape Feature of Test Pieces

After forming grooves as folding lines with a depth of about half the plate thickness using the V-shaped punch tool system, the test piece can be easily bent along a folding line with a gripper, as shown in Figure 9 (mild steel, t = 0.8 mm). The figure shows sharp bending like that in origami can be performed as previously reported [1, 3-6]. Meanwhile, sharp bending is not possible in the case that there is no groove in the test piece, with the radius R of the bending portion being approximately 4 mm as shown in Figure 9(d). It is confirmed that sharp bending was possible for all test pieces after folding line processing using the V-shaped punch tool system.

Next, to examine the projected surface lines of grooved mild steel and aluminum test pieces when using the proposed punch, the angle θ of deviation from the plane after folding line processing was measured using a digital angle measurement device. Table 3 and Figure 10 show that the measured θ is approximately 5° under all conditions of the material and plate thickness range in the folding line processing experiments. This can be explained on the basis of the geometric dimensions as follows.

The height of the V-shaped punch from the bed surface is about 1.4 mm, and the penetration is approximately 0.2–0.4 mm, such that the gap between the surface of a test piece and that of the bed is about 1 mm (Figure 10(b)). The V-shaped punch is located at the center of the bed width of 50 mm. In the case of a test piece having a length of 10 mm or more, the test piece sprung upward and interferes with the bed surface, and should be forced no more deformation during V-shaped punch indentation. It is presumed that the surface of the test piece forms an angle of deviation θ (= 2α) from the original test piece flat surface as approximately 5° (α = gap 1 mm / bed half width of 25 mm × 180° / π = 2.3°) after folding line processing.

It is expected that these characteristics can be considered in the design of a jig and tool system to benefit sharp bending in the subsequent process.

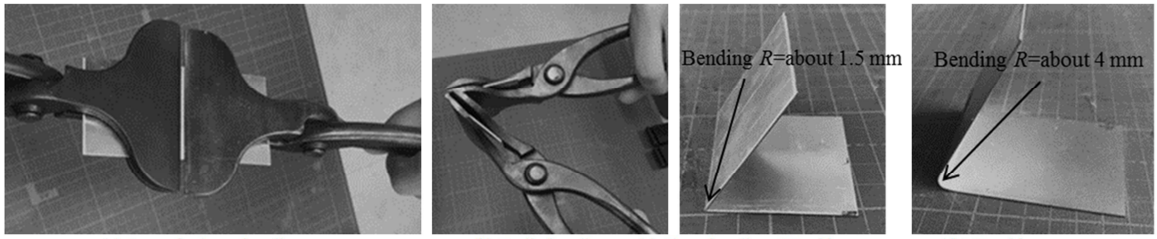

(a) Start of gripper bending (b) Easily bending (c) Sharp bending OK with groove (d) NG without groove

Figure 9. *Bending test for grooved mild steel pieces (t=0.8 mm).*

(a) Measured θ =4.8° of grooved mild steel piece (t=0.8 mm)

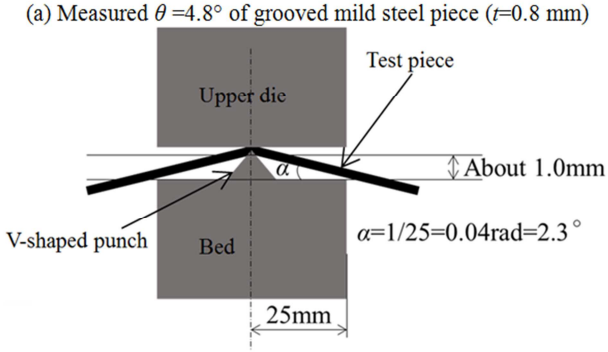

(b) θ=2α based on die dimensions of groove forming by digital angle measurement device

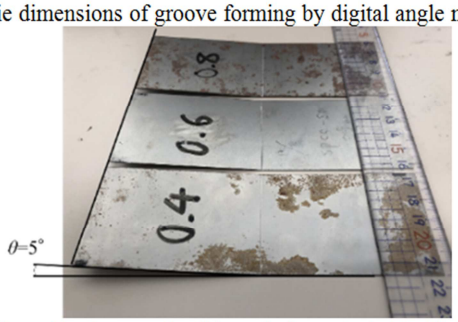

(c) θ=about 5° of grooved mild steel pieces (t=0.4/0.6/0.8 mm)

Figure 10. *Measurement of deflection angle θ from the grooved test piece.*

Table 3. *Measured θ by digital angle measurement.*

Mild steel		**Aluminum**	
***t*(mm)**	***θ*(°)**	***t*(mm)**	***θ*(°)**
0.4	5.3	0.4	5.1
0.6	5.0	0.6	4.9
0.8	4.8	1.0	4.4

4. Discussion

4.1. FEM Model and FEM Analysis Method

There have been many studies on deformation resistance in forging, which was introduced by some reports [12, 13]. However, forging with a V-shaped punch whose tip is arcuated has hardly been investigated except by Ogawa and Makinouchi [1].

The present study performs various FEM analyses of the three-dimensional plate deformation behavior through V-shaped punch indentation. The characteristics of FEM analysis are explained as follows.

Three-dimensional plate deformation through V-shape punch indentation is analyzed. The material constants are given in Table 1. Dies such as the V-shaped punch and bed are modeled as rigid bodies with shell elements and the test piece is modeled as an elastoplastic piece with solid elements as shown in Figures 11 and 12. LS-DYNA [14] is used for FEM analysis. The dynamic explicit analysis method is used for the analysis of deformation until the indentation of the V-shaped punch reaches half thickness and the static implicit analysis method is used for the analysis of the subsequent spring back. The coefficient of friction between the plate and die is set at 0.1.

In the FEM as shown in Figure 11, the plate test piece (having a width of 50 mm, length of 150 mm, and thickness of 1.6, 1.2, 1.0, 0.8, 0.6, and 0.4 mm) is modeled precisely with 100 divisions in width, 8 divisions in thickness, and 225 divisions in length (but 75 divisions for the central part of 8 mm and 150 divisions for other area length 142 mm), finally 180,000 (=100 × 8 × 225) solid elements used. An approximation of a regular octagon is made as shown in Figure 11(c, d) for the center tip shape of the V-shape punch to have R = 0.2 mm. The number of shell elements for the die is 3780. Moreover, FEM models are generated not only for a plate length of 150 mm, which was used in the experiment, but also for a plate length of 6 mm without an upper die as shown in Figure 12 to check for the sprung up phenomenon of the center parts. The number of solid elements for the plate test piece is 60,000 (=100 × 8 × 75) and the number of shell elements for the die is 3612.

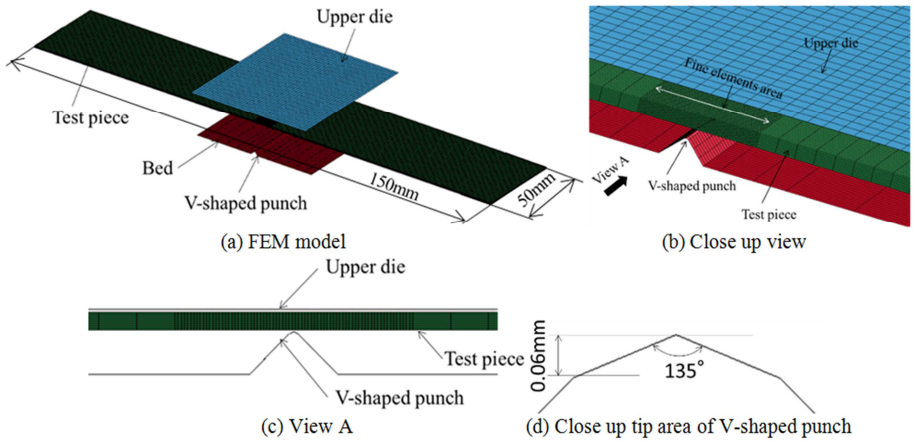

Figure 11. *FEM model for long test piece.*

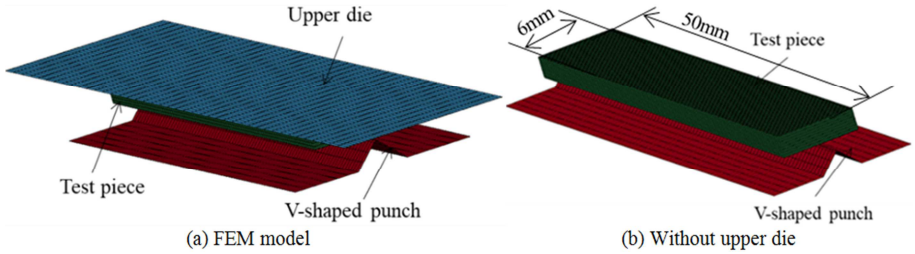

Figure 12. *FEM model for short test piece.*

4.2. Relationship Between V-shaped Punch Indentation and Indentation Load

Figure 13 presents the relationship between the V-shaped punch indentation η and indentation load P obtained from FEM analysis as black/red curves. The corresponding experimental data in Table 2 are presented as square symbols in the figure. P obtained in the FEM analysis using material constants given in Table 1 is 20% to 30% (Figure 13, red curve) lower than the experiment data for mild steel with t = 0.8 mm and aluminum with t = 1.0 mm. The plasticity coefficients are thus changed to fit the relationship between the V-shaped punch indentation η and indentation load P, resulting in F = 750 MPa for mild steel and F = 240 MPa for aluminum (black lines in Figure 13). There is a small difference between the FEM results and experiment data in the case of the thinnest t = 0.4 mm. There is good agreement in the case that the thickness exceeds t = 0.4 mm. The error in the FEM analysis is higher for the thinnest t = 0.4 mm for the following reasons. The dies and punch are rigid bodies in the FEM and do not deform, whereas real dies and punches are made from steel, which elastically deforms under load. Complex nonlinear deformation behavior is strongest for t = 0.4 mm because the volume fraction occupied by the V-shaped punch tip arc in the plate is greatest in this case.

The indentation is denoted by η in verifying the FEM results based on the experimental data. η = 0 is the indentation starting point as shown in Figure 5. In the case of a punch tip arc R = 0.2 mm, Figure 5 shows that the punch tip arc is indented in the range η = 0–0.06 mm, finally after that the inclined 90° punch surface is indented in the range $\eta \geq 0.06$ mm. The relationship between λ_s and η is thus expressed as

$$\eta = 0.2 - \sqrt{0.2^2 - \left(\frac{\lambda}{2}\right)^2} \quad for\ \eta = 0 \sim 0.06mm \tag{1}$$

$$\eta = \lambda_s / 2 - 0.08 \quad \text{for } \eta \geqq 0.06 \text{ mm} \tag{2}$$

Until the completion of the initial stage (i.e., the completion of the V-shaped punch tip arc indentation), the load increment ratio (= load/indentation) is large. After this stage, the value of P required for indentation to half the plate thickness is almost proportional to η as seen in the FEM results and experiment data for mild steel and aluminum in Figure 13. The proportionality coefficient K is 1282.8 MPa for mild steel and 400.9 MPa for aluminum. The intercept value of the proportional approximation formula is approximately 0.1K.

Using the approximation formula P = 1282.8η + 132.0 obtained from measurements of mild steel in this paper, P = 1158 N/mm is estimated as the load required to indent to half the thickness t =1.6 mm at η = 0.8 mm. This estimated value is almost the same as measured load P as indenting to half the thickness mild steel t =1.6 mm at η = 0.8 mm with a punch tip arc R = 0.2 mm by Ogawa and Makinouchi [1].

The reason why P as the panel half-thickness indentation load for the V-shaped punch is largely proportional to η is that the compression strain distribution due to V-shaped punch indentation is similar for each plate thickness when ignoring the nonlinear behavior of the punch tip arc, and the

compression stress distribution is therefore almost the same for each panel thickness. The projected area of the V-shaped punch indentation increases in proportion to the plate thickness, and the indentation load P thus increases almost in proportion to η. The ratio of the indentation load P for mild steel/aluminum becomes 3.20 (=1282.8 MPa/400.93 MPa). The plasticity coefficient F, which greatly affects the deformation resistance, is changed to adapt the FEM results to the experimental data. As a result, the F ratio of mild steel to aluminum becomes 3.12 (=750 MPa/240 MPa), which is nearly 3.20.

Before changing F, the initial F ratio of mild steel to aluminum in Table 1 is 4.10 (= 627 MPa/153 MPa). There is a large difference between the initial ratio of 4.10 and the final ratio of 3.20. Meanwhile, both the ratio of the Young modulus as mild steel to aluminum and that of the 0.1% yield strength as mild steel to aluminum are 2.94 (= 206 GPa/70 GPa), which is close to 3.20. The strain hardening index n has the same value for mild steel and aluminum. It is therefore confirmed that changing F is an effective approach. A study on the effect of other material constants is left as future work. The proportionality coefficient K of the indentation load per unit length of the folding line P to η is 1.7 times the plasticity coefficient F for mild steel and aluminum (= 1282.8/750, = 400.93/240).

These equations allow approximate calculations to be made in determining the proper load for folding line processing from the total length of all folding lines on the product to be pressed. However, future work will need to adopt more materials. It is thus considered appropriate to estimate plate deformation behavior during V-shaped punch indentation in an FEM analysis. Next, the mechanism of the surface imprint length formed by V-shaped punch indentation should be considered on the basis of FEM results.

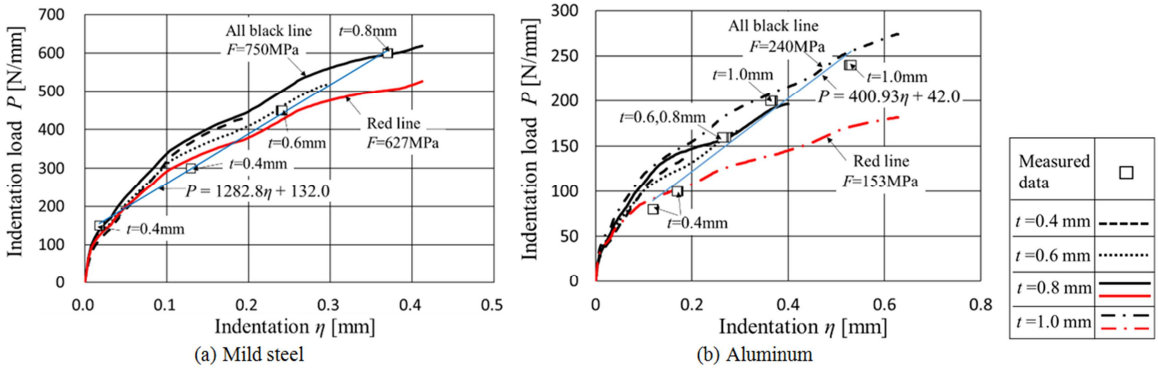

Figure 13. *Comparison between measured data and indentation load curves by FEM analysis.*

4.3. Surface Imprint Length by V-shaped Punch Indentation

Figure 14 presents the FEM results of the plate deformation behavior in the vicinity of the V-shaped punch during indentation in mild steel and aluminum plates having a length of 6 mm, width of 50 mm, and thickness t = 0.8, 1.2, and 1.6 mm.

The figure also shows the deformation behaviors of the plates and expansion of the equivalent plastic strain distribution in four evenly spaced stages until the indentation of the V-shaped punch reaches the plate half thickness (100% stage) for mild steel with t = 0.8 mm. Die models are not included in the figure, such that the side view is clearer. Indentation to the 25% stage results in the equivalent plastic strain reaching the back side of the plate and the spread of the equivalent plastic strain on the approach side. Indentation to the 50% stage results in large growth of the plastic region and the plate surface leaving the bed and springing up at the boundary between the plastic strain region and elastic region. Indentation to the 100% stage results in the largest spring up angle. The color levels for the equivalent plastic strain distribution used in this figure are used in the following figures. Figure 15 shows the equivalent plastic strain distributions and deformation shapes at the 100% stage in the cases of mild steel (t = 0.8, 1.2, and 1.6 mm).

There are common characteristics in these cases such that the normal extending representative action line as the distributed load at the slope surface of the concave part formed by the V-shaped punch indentation reaches the sprung up position of the plate back surface. There is effective plastic strain between the left and right sprung up positions. Outside this area, there is no surface imprint because there is no effective plastic strain. Additionally, the interval between the left and the right sprung up positions is presumed to be the surface imprint length λ_b on the plate back surface measured in the folding line processing experiments. η_b represents the surface imprint length of the back side of the plate in FEM analysis, η_b is about 2.0–2.2 times the plate thickness, which is similar to the experiment measured data.

Figure 15 shows that there is almost no difference in the deformed shape and the equivalent plastic strain distribution with a changing plasticity coefficient F between the cases of mild steel and aluminum. That is to say, they are strongly affected by the geometric conditions of the V-shaped punch indentation, not depended on the plate materials.

Figure 16 shows FEM results for the three principal stress distributions at the 100% stage of indentation for mild steel (t = 0.8/1.2/1.6 mm). The first principal stress is high tensile stress in the length direction, the second principal stress in the width direction is negligibly small, and the third principal

stress is large compressive stress (negative) in the thickness direction. These distributions are generally symmetrical vertically in the thickness direction.

Figure 17 and Table 4 show the transition of the sprung up angle γ due to the V-shaped punch indentation and the spring back angle $\Delta\gamma$ after unloading in FEM analysis. The sprung up angle γ is inversely proportional to the plate thickness. As mentioned above, because the compressive load per unit area should be the same for each panel thickness, the change in angle γ due to the compressive load is inversely proportional to the stiffness by thickness. Moreover, in each case, because of the complete plastic deformation around the plate center and the spring back angle $\Delta\gamma$ being as small as 0.1 degree, the spring back in folding line processing using the V-shaped punch can be neglected. This is explained as follows.

Both the effective plastic strain distributions and three principal stress distributions (Figures 15 and 16) are generally symmetrical vertically in the thickness direction, and both the stresses inside and outside the bending area are the tensile side and are close to being uniform. Therefore, the spring back should be suppressed.

It is difficult to conduct experiments for the sprung up phenomenon using a test piece with a length of 6 mm and the proposed V-shaped punch, because the punch height is only 1.4 mm as shown in Figure 4. But Ogawa and Makinouchi [1] reported that the measured sprung up angle γ was about 5° and that spring back could be ignored for mild steel with thickness of 1.6 mm in experiments using their very high punches with a punch tip arc R = 0.2 mm as shown in Figure 2. The FEM results reported in the present paper are thus validated by their report.

Next, FEM results for the experimental conditions are explained as follows. FEM analyses are performed to clarify plate deformation behaviors for the V-shaped punch indentation of mild steel and aluminum having a length of 150 mm, width of 50 mm, and thickness t = 0.4, 0.6, 0.8, and 1.0 mm. Figure 18 shows the deformed plate shape around the V-shape punch and effective plastic strain enlargement.

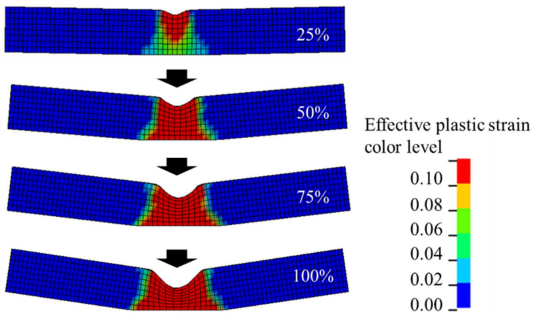

Figure 14. *Effective plastic strain enlargement process in the case of mild steel, 6 mm length, t=0.8 mm, η=0 ~0.5t by FEM analysis.*

Figure 18 shows plate deformation behaviors and the expansion of the equivalent plastic strain distribution in four evenly spaced stages until the V-shaped punch reaches the plate half thickness (100% stage) for mild steel thickness of 0.8 mm and a side view with no die model. Different from Figures 14 and 15, the sprung up angle is forcibly suppressed because the plate length of 150 mm is so long that the striking bed stops its deformation as shown in Figure 10(b).

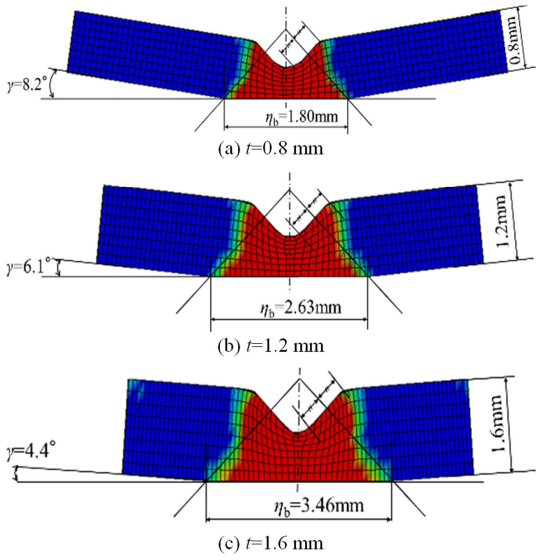

Figure 15. *Effective plastic strain distributions at η=0.5t for mild steel, 6 mm length, t=0.8/1.2/1.6 mm by FEM analysis.*

Table 4. *Sprung-up angle γ and spring back angle Δγ at η = 0.5t.*

Material	t (mm)	γ(°)	$\Delta\gamma$(°)
Mild steel	0.8	8.2	0.12
	1.2	6.1	0.12
	1.6	4.4	0.09
Aluminum	0.8	8.1	0.09
	1.2	5.9	0.09
	1.6	4.2	0.07

As in Figures 14 and 15, the effective plastic strain region reaches the plate back surface and spreads with a V-shape punch indentation beyond the 25% stage. However, it is a characteristic difference that this forcible suppression in Figure 18 spreads the effective plastic strain region around the concave surface in the length direction more than what is seen in Figures 14 and 15.

Additionally, as in Figure 15, beyond the 50% stage, the plate sprung up on the boundary line between the plastic region and elastic region. The sprung up angle is about 2.5° (Figure 19(d)) for each plate thickness because the plate warping angle is approximately θ = 5° (= 2.5° for one side × 2) at the 100% stage as shown in Figure 10(b). In this way, the warped angle is decided by the geometric relations among such design dimensions as the bed size, punch height, plate length, and sprung up angle. Folding line processing using the proposed V-shape punch can be conducted to realize the target θ by adjusting these design dimensions.

Figure 19 shows the effective strain distributions and deformation shapes at the 100% stage of indentation for the mild steel (t = 0.4, 0.6, 0.8 mm) and aluminum (t = 1.0 mm).

There is a small difference in the angle deformation pattern between plate lengths of 150 and 6 mm. However, there is a common characteristic as follows.

The sprung up positions on the plate back surface are determined by the normal extended representative action line

from the center of the concave surface as the load distributed by the V-shaped punch indentation. In the case of a plate length of 150 mm, the surface imprint length η_b obtained in FEM analysis is 2.0–2.2 times the plate thickness. Although all die models in the FEM analysis are rigid bodies and thus do not deform, the plate back surface is a little convex in shape as shown in the experiment photograph presented in Figure 7(a). It is estimated that the plate back surface deforms to be a little convex in shape owing to the upper die being a little concave in shape (50 mm × 50 mm × 100 mm) because it is made of hard steel and is not a rigid body. It is therefore deduced that the upper die, being slightly concave, has deformation of about 0.1 mm as calculated using the following approximation equations and the plate back surface, being slightly convex, has the same deformation as seen in the side view photograph in Figure 7(a).

Compressive stress of the upper die =30 kN / (surface imprint length of approximately 2 mm × plate width of 50 mm) = approximately 300 MPa.

Concave deformation of the upper die = Compressive strain of 0.0015 (= compressive stress 300 MPa/Young modulus 206 GPa) × thickness of 50 mm = approximately 0.1 mm.

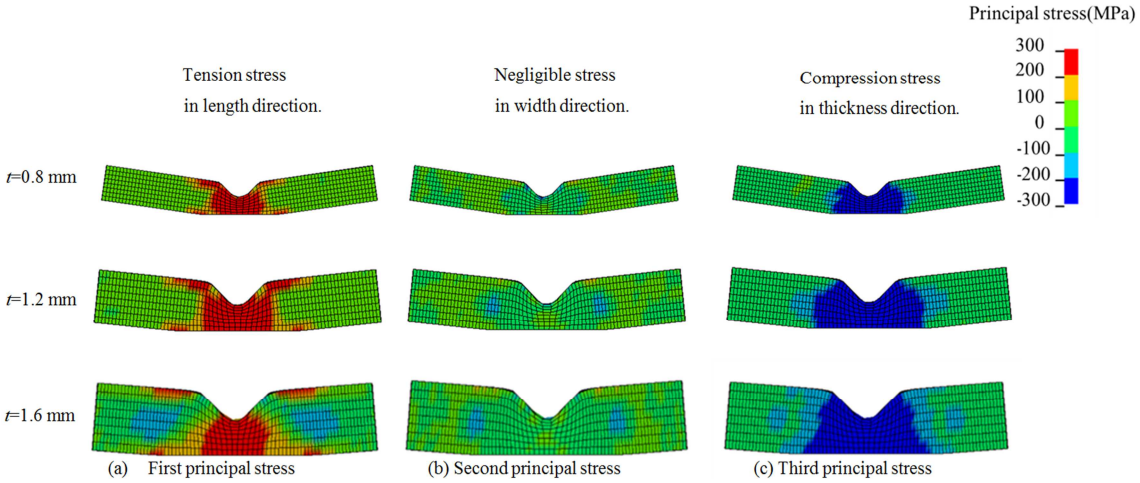

Figure 16. *Three principal stress distributions at η=0.5t for mild steel, 6 mm length, t=1.6/1.2/0.8 mm by FEM analysis.*

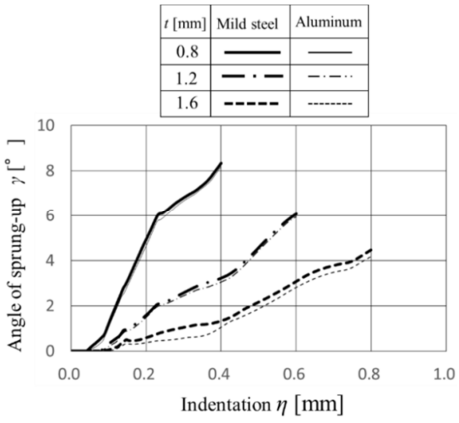

Figure 17. *Effective plastic strain distributions at η=0.5t.*

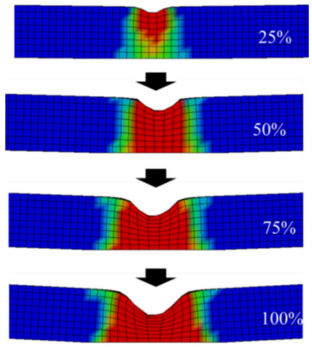

Figure 18. *Effective plastic strain enlargement process in the case of mild steel, 150 mm length, t=0.8 mm, η=0 ~0.5t by FEM analysis.*

4.4. Relationship Between V-shaped Punch Geometry and Surface Imprint Length

As the V-shaped punch indentation reached half thickness, it is clear from the FEM analysis that boundary lines form between a region of plasticity inside the concave slope surface and a region of elasticity outside. The position of the boundary line on the plate back surface matches the plate sprung up position determined by the normal extending representative action line from the center of the concave slope surface formed by V-shaped punch indentation to the plate back surface. These phenomena as plasticity deformation suppress the sprung up deformation. The FEM results suggest that the distance between the left and right boundaries of the plastic/elastic region is equal to the surface imprint length on the plate back surface. The relation between the V-shaped punch shape and the surface imprint length should be considered on the basis of the geometric calculations.

Now, as shown in Figure 20(a), when the V-shaped punch EAC without tip arc *R* penetrates to half thickness (0.5*t*), the distance between position I and its opposite position H is 2*t*.

Position I is determined by the normal extending representative action line from position D (the center of the concave slope surface). It is clear from this figure that the geometric relation of the distance HI = 2*t* mm is almost constant even though the entered point of the V-shaped punch EAC is a little deeper or shallower than the half thickness.

Next, as shown in Figure 20(b), as the V-shaped punch DAD with tip arc R = 0.2 mm indents to half thickness (0.5t), the distance between positions I and H is equal to 2(t + 0.14). Because triangles CBF and OA′O′ are congruent, Figure 20(a) also shows that the geometric relationship of the distance HI = 2(t + 0.14) does not change before and after the V-shaped punch indentation to half thickness. So, the V-shaped punch indentation to half thickness (0.5t) results in a clear sprung up phenomenon.

Therefore, the plastic strain region on the plate back surface can be formed through indentation with a V-shaped punch. The surface imprint length is equal to 2(t + 0.14) on the basis of the geometric relationship in the case of a V-shaped punch with tip arc R = 0.2 mm. Figure 21 shows the comparison with the measured surface imprint length λ_b in Table 2, the six FEM results for η_b in Figures 15 and 19, and the geometric calculation results. Even, FEM analysis has many analysis conditions such as modeling methods, analysis methods, test piece dimensions accuracy, material constants, etc., η_b well matches the geometric calculation results. It is seen that η_b strongly depends on the geometric conditions. Although there are sources of error, such as die deformation, λ_b matches the geometric calculation results well.

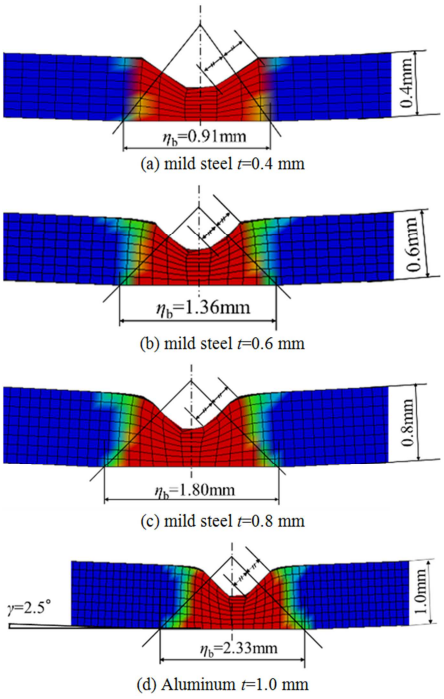

Figure 19. *Effective plastic strain distributions at η=0.5t for mild steel t=0.4/0.6/0.8 mm, aluminum t=1.0 mm, 150 mm length by FEM analysis.*

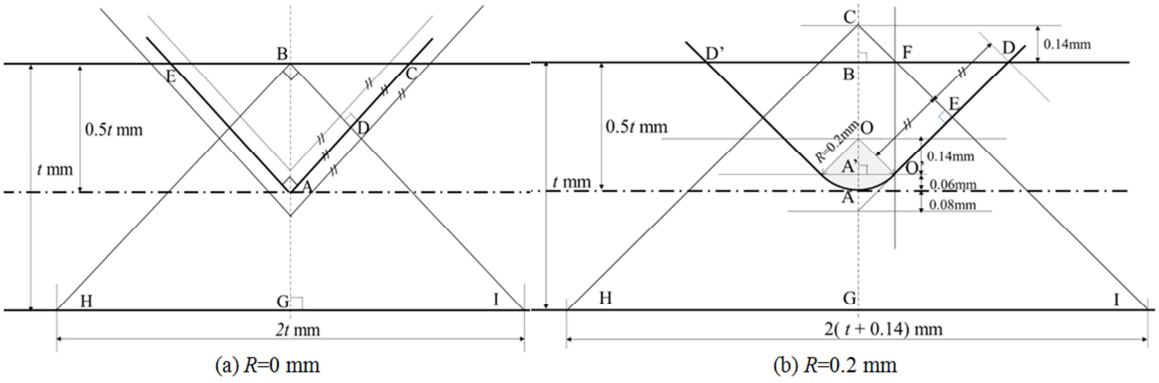

Figure 20. *Geometry of V-shaped punch in half thickness indentation of plate.*

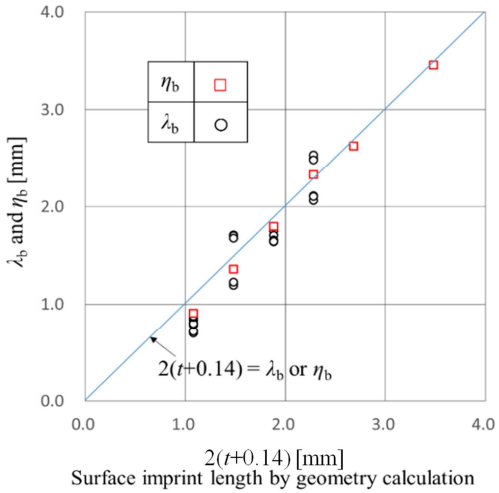

Figure 21. *Comparison between surface imprint length of measured data, λ_b, FEM results η_b and that of geometry calculation.*

4.5. FEM Analysis and Experiment Verifications for Terminal Effect of V-shaped Punch

The case of intersection folding lines inside the panel surface is beyond the scope of this paper because of the risk of human injury. The intersection of folding lines in this paper is near the plate cutting lines. Figure 6 shows the intersection of three folding lines around the plate cutting lines of a product. The distance L from the V-shaped punch terminal to the plate folding lines is 0.8 mm by design for FL-2. Here, the effect of the distance L on the terminal effect is verified by FEM and experiment al results. To investigate the three-dimensional plate deformation around the V-shaped punch terminal in this study, FEM analyses for the four cases that L =1.0, 0.8, and 0.5 mm (denoted L1.0, L0.8, and L0.5) and L is rather far (abbreviated L far) with a solid element size for the panel finer than that in Figure 11 are performed as shown Figure 22. Each effective strain distribution is

obtained from FEM results for the state that the indentation of the V-shaped punch reaches the half thickness of aluminum test pieces with t = 1.0 mm as the product shown in Figure 6.

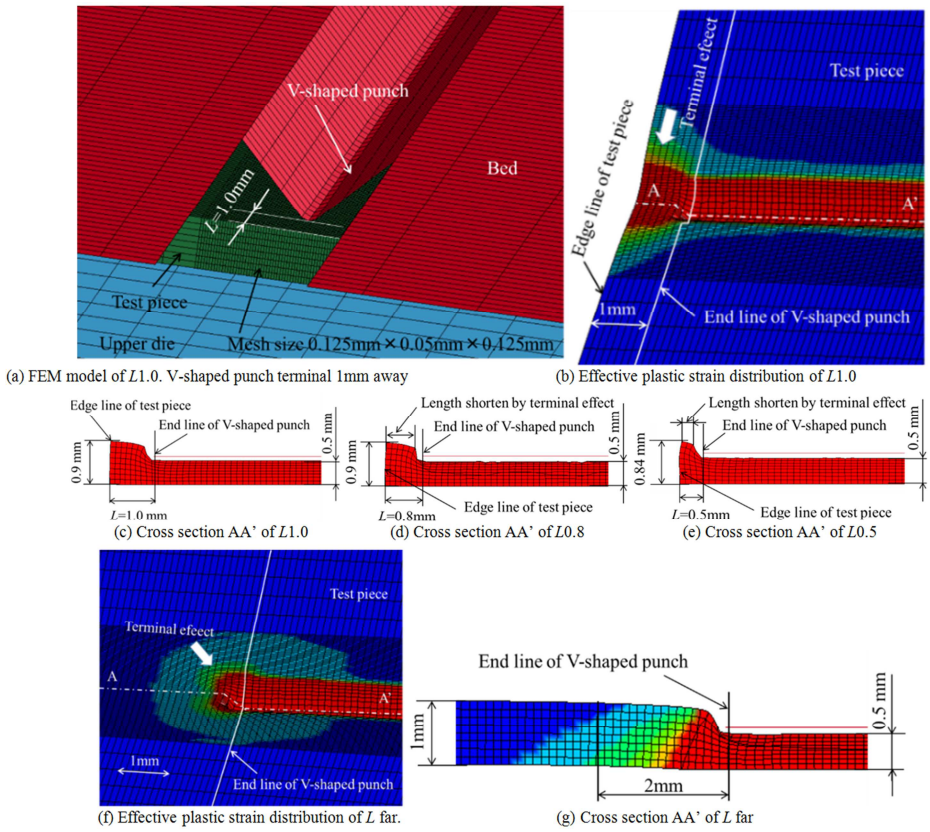

(a) FEM model of L1.0. V-shaped punch terminal 1mm away
(b) Effective plastic strain distribution of L1.0
(c) Cross section AA' of L1.0
(d) Cross section AA' of L0.8
(e) Cross section AA' of L0.5
(f) Effective plastic strain distribution of L far.
(g) Cross section AA' of L far

Figure 22. *Three dimension deformation behavior around terminal of V-shaped punch by FEM analysis.*

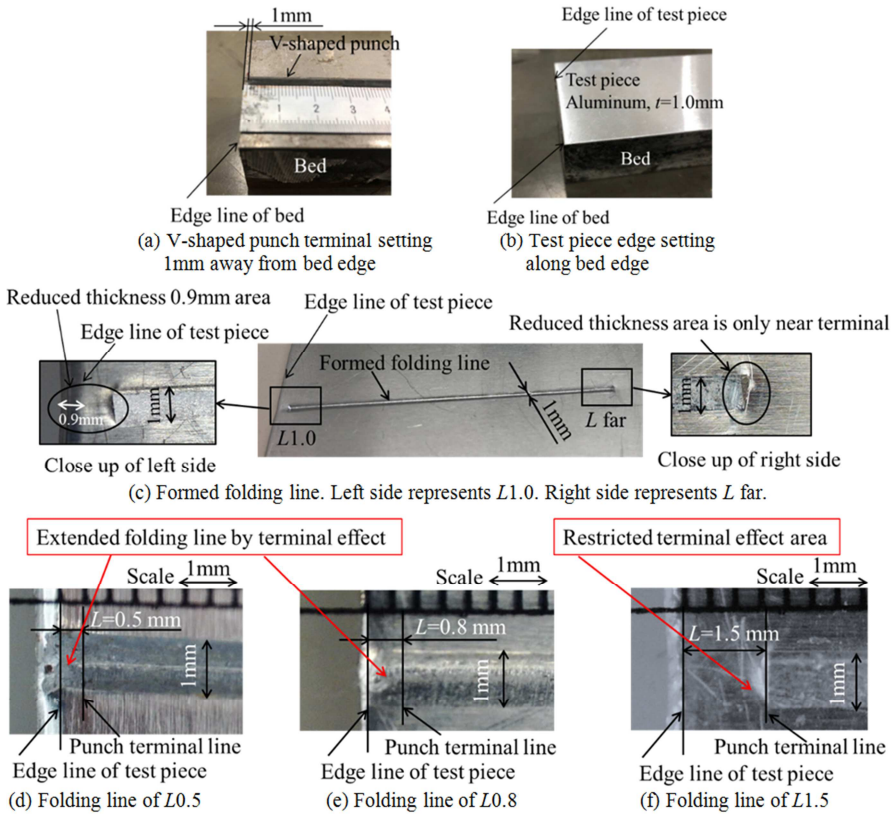

(a) V-shaped punch terminal setting 1mm away from bed edge
(b) Test piece edge setting along bed edge
(c) Formed folding line. Left side represents L1.0. Right side represents L far.
(d) Folding line of L0.5
(e) Folding line of L0.8
(f) Folding line of L1.5

Figure 23. *Experimental verification of V-shaped punch terminal effect. FEM results in Figure 22 confirmed by experiments.*

In the case of $L1.0$, the thickness reduction of 0.1mm in the plate thickness of 1.0 mm means that the effective plastic strain exceeds 10%. There is thus the terminal effect in an axial region of 1.0 mm where the V-shaped punch does not reach as shown in Figures 22(b) and 22(c). $L0.8$ and $L0.5$ have similar characteristics in that deformation shortens the axial surface length of the test piece more than in the case of $L1.0$. As a result, folding lines extend from the V-shaped punch terminal in the axial direction owing to the terminal effect as shown in Figures 22(d) and 22(e).

In the L far case, deformation extends to about 2 mm in the axial direction gradually weakening so that the plastic region where the thickness reduction of 0.1 mm region is limited to the vicinity of V-shaped punch terminal as shown in Figures 22(f) and 22(g). These FEM results are experimentally verified in the following procedure as shown in Figure 23.

1) The V-shaped punch is set on the bed such that the gap is 1.0 mm from the V-shaped punch terminal to the bed edge as shown in Figure 23(a).
2) The aluminum test piece (t =1.0 mm), sufficiently longer than the V-shaped punch, is set on the bed aligning test piece edge with the bed edge as shown in Figure 23(b).
3) The upper die (Figure 4) is set and folding line processing is performed by applying an indentation load P = 242.5 N/mm (Figure 13(b)), which is calculated using the proportional approximation formula.
4) The folding line is formed such as in Figure 23(c). The left end of the folding line represents $L1.0$ and the right end represents L far.
5) The enlarged photograph (Figure 23(c)) at the left end of the folding line shows that the 1.0 mm region from the V-shaped punch terminal to the test piece edge is recessed relative to the surrounding area. The caliper measurement of the plate thickness in this area is 0.9 mm, which means that there is a plasticity deformed area with a thickness reduction of 0.1 mm in the plate thickness of 1.0 mm.
6) The enlarged photograph (Figure 23(c)) at the right end of the folding line shows that plastically deformed region with reduced thickness is limited to the vicinity of the V-shaped punch terminal.
7) When the folding line processing experiments are performed under different conditions by changing the distance L between the V-shaped punch terminal and plate cutting lines using gap gauges (0.5, 0.8, and 1.5 mm), folding lines are formed around the plate cutting lines as shown in the photographs (Figures 23(d), (e), (f)).

The FEM analysis and experimental verification of the terminal effect of the V-shaped punch show that, when the distance L between the V-shaped punch terminal position and plate cutting line exceeds 1.0 mm (Figures 23(c), (f)), the grooving depth of folding lines extended in the axial direction by the terminal effect is shallow and not clear as the depth is only approximately 0.1 mm. In the case that $L \leq 0.8$ mm, however, the folding line extended by the terminal effect (Figures 23(d), (e)) is sharp in the axial direction relative to the plate cutting line.

As mentioned above, although the length that the V-shaped punch cannot reach because three V-shaped punches intersect around the plate cutting line is about 0.8 mm for the product in Figure 6, it is reasonable that the folding lines can be extended in the axial direction by the terminal effect such that they become almost continuous and sharp bending is possible.

5. Conclusion

The contributions and results of the present study are summarized as follows.

(1) A V-shaped punch was proposed to be applied easily at low cost for origami forming products with many folding lines and the intersection of multiple folding lines. This method is highly efficient, at least in experiments and for prototype products.

(2) The corner R of the V-shaped punch is finished to be as small as 0.2 mm after cutting out a high-speed steel block to a cross section size of 2 mm × 2 mm. This size is the minimum that can be achieved by milling. The V-shaped punch is set inside a 2.8 mm wide × 1.4 mm deep groove that is formed by a V-shaped cutter. There is a region (of about 0.8 mm) that a punch having a width of 2.8 mm cannot reach because of the interference of three V-shaped punches crossing neighboring plate cutting lines. However, sharp bending is possible using the folding lines extended along the axial direction owing to the terminal effect of the V-shaped punch. Verifications were carried out in FEM analysis and experiments.

(3) It was shown that the indentation load required for the V-shaped punch to penetrate to half thickness is almost proportional to the indentation η based on experiments and FEM analysis. In the cases of mild steel and aluminum, the proportional coefficient K of the indentation load P per unit folding line length and indentation η is about 1.7 times the plasticity coefficient F. The intercept value of the proportional approximation formula is approximately $0.1K$. This relationship makes it possible to estimate the proper load from the total length of folding lines on the applicable products.

(4) FEM results showed that the normal extended representative action line from the center of the concave slope surface formed by the V-shaped punch indentation to the plate back surface matches the plate sprung up positions. It was also found that the effective plastic strain region is between the left and right sprung up positions. The elastic strain region expands outside this region. It is confirmed that this interval length matches the surface impression length on the plate back surface measured in experiments.

(5) The geometric calculation results based on the above proposed mechanism correspond to experimental and FEM results for the surface imprint length on the plate back surface for indentation of the V-shaped punch to half thickness. Therefore, the plate deformation behavior of the V-shaped punch indentation strongly depends on the geometry.

(6) The proposed method provides many findings and shows the effective method by measurement of λ_s and λ_b from photographs, recognizing the groove depth and the plate deformation behavior. The method of obtaining λ_s and λ_b by making measurements from photographs and considering the mechanism is recommended as overcome solution in the case of having troubles for sharp bending and origami forming by using this proposed method. As an example, when sharp bending cannot be performed properly owing to a shallow groove of a folding line, the real condition for folding line processing can be reconsidered using measurements from photographs of the defective formed plates as performed in this paper.

6. Future Work

Future work directions of research are 1) to study proper conditions for folding line processing with different types of material, 2) to study the relationship between the indentation load and V-shaped punch indentation using plasticity coefficient, strain hardening index and yield stress, 3) to study the shape and dimensional allowable accuracy of bent products after folding line processing, and 4) to devise a method of automatic bending to be applied after folding line processing.

References

[1] Ogawa, H. and Makinouchi, A., Sharp bending of sheet metal with indentation of V-shaped punch, Journal of the Japan society for technology of plasticity, Vol. 40, No. 459 (1999), pp. 338-342 (in Japanese).

[2] Nguyen, T. T. H., Terada, K., Tokura, S. and Hagiwara, I., Development of origami forming to improve the flexibility of truss core panel design, Transactions of the JSME (in Japanese), Vol. 80, No. 819 (2014), DOI: 10.1299/transjsme.2014smm0314.

[3] Terada, K., Tokura, S., Sato, H., Makita, A. and Hagiwara, I., Evaluation of the Bending Stiffness on Assembled Light Weight and High Strength Panel, Transactions of the JSME (in Japanese), Vol. 81, No. 828 (2015), DOI: 10.1299/transjsme.15-00039.

[4] Terada, K., Tokura, S., Takahashi, T. and Hagiwara, I., Practical Development of ATCP (Assembly truss core panel), RESEARCH REPORTS National Institute of Technology, Fukushima College, Vol. 58 (2017), pp. 1-8 (in Japanese).

[5] Terada, K. and Hagiwara, I., Freely manufacturing methods such as origami forming, Journal of the Japan Society of Mechanical Engineers, Vol. 119, No. 1175 (2016), pp. 564-565 (in Japanese).

[6] Terada, K., Deformation mechanism in Gripper bending process, Bulletin of the Japan society for technology of plasticity, Vol. 1, No. 3 (2018), pp. 195-199 (in Japanese).

[7] Tokura, S. and Hagiwara, I., Forming process simulation of truss core panel, Transactions of the Japan Society of Mechanical Engineers, Series A, Vol. 74, No. 746 (2008), pp. 1379-1385 (in Japanese).

[8] Tokura, S. and Hagiwara, I., Forming Process Simulation of Truss Core Panel, Journal of Computational Science and Technology, Vol. 4 (2010), No. 1, pp. 25-35 (Release Date: March 30, 2010).

[9] Tokura, S. and Hagiwara, I., A Study for the Influence of Work Hardening on Bending Stiffness of Truss Core Panel, J. Appl. Mech., Vol. 77/031010-1-031010-6(2010-5).

[10] Abe, A., Terada, K., Yashiro, H. and Hagiwara, I., Characteristics of truss core created by origami forming method, Proceedings of the ASME 2019 IDETC/CIE 2019.

[11] Abe, A., Yashiro, H. and Hagiwara, I., Development of vertical incident sound insulation simulation technology using finite element method and application to lightweight core, Transaction of the JSME (in Japanese), Vol. 86, No. 891 (2020), DOI: 10.1299/transjsme.20-00126.

[12] Toda, M., Research on deformation resistance of steel under forging conditions, Osaka University Doctoral Thesis Graduate School of Engineering and Science (1999) (in Japanese).

[13] Yoshida, Y., and Ishikawa, T., Evaluation Tests of Flow Stress and Workability in Forging, Journal of the Japan society for technology of plasticity, Vol. 50, No. 577 (2009), pp. 93-97 (in Japanese).

[14] Livermore Software Technology Corporation, LS-DYNA User's Manual (Version R7.0) (2014), JSOL Corporation (in Japanese).

[15] Nagata, S. and Yanagimoto, J., Fundamentals in Metal Forming (revised Edition) (1997), p. 22, CORONA PUBLISHING CO (in Japanese).